

# Towards In-Vivo X-Ray Nanoscopy

## The Effect of Motion on Image Quality

Leonid Mill<sup>1</sup>, Bastian Bier<sup>1</sup>, Christopher Syben<sup>1</sup>, Lasse Kling<sup>2</sup>,  
Anika Klingberg<sup>3</sup>, Silke Christiansen<sup>4,5</sup>, Georg Schett<sup>3</sup>, Andreas Maier<sup>1</sup>

<sup>1</sup>Pattern Recognition Lab, Friedrich-Alexander-University Erlangen-Nuremberg

<sup>2</sup>Max Planck Institute for the Science of Light, Erlangen

<sup>3</sup>Institute of clinical Immunology, University Hospital Erlangen

<sup>4</sup>Freie Universität Berlin, Berlin

<sup>5</sup>Helmholtz Zentrum Berlin für Materialien und Energie, Berlin

leonid.mill@fau.de

**Abstract.** Novel X-Ray Microscopy (XRM) systems allow to study the internal structure of a specimen on nanoscale. A possible use of this non-destructive technology is motivated in the medical research area. *In-Vivo* investigation of medication over a period of time and its effects on perfusion and bony structure might lead to a better understanding of drug mechanisms and diseases like Osteoporosis and could lead to new approaches to their treatment. The first step towards *in-vivo* XRM imaging is to investigate the suitability of recent XRM systems for this task and subsequently to determine the system parameters. In this context, the impact of mice motion on the image quality is studied in this work. This paper aims to simulate the effects of breathing motion and muscle relaxation of the mice on the reconstructed images, which already effects the projection images. We therefore assume a mouse's respiration motion pattern, which happens four time during a single projection acquisitions, and the muscle relaxation movement due to anesthesia and simulate its impacts on image quality. Additionally, we show that a frame rate of at least 16 fps is needed to capture *in-vivo* movements in order to apply state-of-the-art motion correction methods.

## 1 Introduction

X-Ray Microscopy (XRM) systems are used in a variety of research areas including material sciences, medicine, and biology. One of the benefits of this technology in comparison to recent medical computed tomography (CT) applications is the high resolution of the reconstructed images with a voxelsize of up to 700 nm. This permits the investigation of structures in nano-scale in a non-destructive manner. One of these applications is the acquisition of mice bones in order to investigate the inner bony structures. We aim at the investigation *in-vivo* in order to detect effects of medication on the bone structure. In theory, the resolution that can be achieved with such system is sufficient. However, XRM systems are not designed to scan live moving objects such as mice. Despite of

anesthesia, motion due to breathing and the relaxation of their muscles occurs during the scan. In general, motion in CT or CBCT has been investigated in various different applications [1, 2, 3]. However, combined with current exposure times in XRM of 1 s, motion blur appears in each single projection image since mice can breath up to four times during the acquisition of a single image. Furthermore, a whole acquisitions takes more than one hour resulting in motion artifacts in the reconstructions. This decreases the image quality remarkably and makes the evaluation of the medication hardly measurable.

In this work, we investigate the expected effect of this specific mouse movement on the image quality of the projections and the follow up reconstructions. Therefore, we evaluate on the one hand the effect of the exposure time on the projection images. On the other hand, we study the influence of different motion assumptions of the mouse and their influence on the reconstructions. We conduct experiments with different exposure times and discuss, what kind of motion would be observed. We evaluate the results using the Structural Similarity (SSIM) to measure the image quality.

## 2 Materials and methods

### 2.1 Experimental Setup

The simulation study is based on a scan of a high quality reconstruction of a mouse’s tibia, acquired without any influence of motion. These scans have been acquired on a Xradia Versa 520 XRM system using 2000 projection images with an angular increment of  $0.18^\circ$ . The mouse is placed on a rotating plate. The detector size of the system is  $2024 \times 2024$  pixels with a pixel size of  $1.34 \mu\text{m}$ . The resulting reconstructed volume had a size of  $1980 \times 2024 \times 1999$  voxel with an isotropic resolution of  $1.35 \mu\text{m}$ . Note, that this system has currently an exposure time of 1 s per projection, which is very long compared to current medical CT or CBCT systems. The same settings are used to create projection images using CONRAD [4]. For reconstruction, we used a standard FDK back-projection algorithm that consists of a cosine weighting [5], Parker redundancy weighting [6], Ram-Lak ramp filtering [5], and a backprojection step [7]. The voxel size of the reconstructions are set to  $1.34 \mu\text{m}$ .

### 2.2 Occurring mouse motion

To model the mouse motion we consider two different kinds of motion. On the one hand we assume a breathing motion with 240 breathing cycles per minute. During one breathing cycle, an overall motion of  $5 \mu\text{m}$  in the plane horizontal to the ground is assumed, which is defined in the  $x$ - $y$  plane in the following. On the other hand, a second motion is considered as a result of muscle relaxation that appears horizontal to the  $x$ - $y$ -plane with a total motion of  $10 \mu\text{m}$  per hour. This motion is modeled as a linear movement in the  $z$ -direction. These motion assumptions are based on long term experiences of mice under anesthesia. If

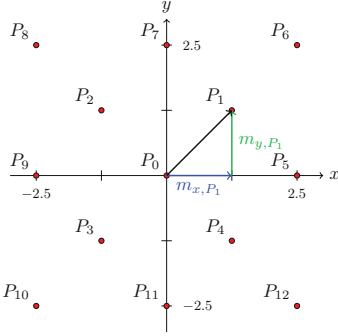


**Fig. 1.** Simulation of the respiration movement by shifting the volume to several points  $P_k$  in the  $x$ - $y$  plane. For each point at a time  $t_j$  a projection is performed and the average over  $k$  projections is computed.

we combine this motion pattern with the current system's exposure time of 1s, we observe four breathing cycles and a relaxation motion of  $\frac{1}{360}$   $\mu m$  per acquired projection image. Thus, the breathing motion results in a motion blur effect in the acquired projections, which is an intra-scan motion, while the relaxation motion, which as inter-scan motion, leads to motion artifacts in the reconstruction. The model for breathing and the relaxation motion are described separately in the next sections.

### 2.3 Inter-scan motion

The relaxation motion is modeled as rigid object transformation in  $z$ -direction that can be incorporated into the projection matrices. For this we multiply to the  $j$ -th projection matrix  $\mathbf{P}_j \in \mathbb{R}^{3 \times 4}$ , with  $j \in \{1, \dots, n\}$ , the respective motion matrix  $\mathbf{M}_j \in \mathbb{R}^{4 \times 4}$  from the right side, yielding a motion corrupted projection matrix  $\mathbf{P}'_j$

$$\mathbf{P}'_j = \mathbf{P}_j \cdot \mathbf{M}_j = \mathbf{P}_j \cdot \begin{pmatrix} 1 & 0 & 0 & 0 \\ 0 & 1 & 0 & 0 \\ 0 & 0 & 1 & m_z^j \\ 0 & 0 & 0 & 1 \end{pmatrix}$$

where  $m_z^j$  indicates the movement based on muscle relaxation.

### 2.4 Intra-scan motion

Based on the assumptions stated above, reconstructions are created from motion blurred projections. The effect of the long exposure time can be seen as the average of several projections with variable translations. For the simulation we assume a movement of a maximum of 5  $\mu m$  in a single breathing cycle and four breathing cycles per second. Thus, the different respiration motion states during the acquisition of one single projection image can be modeled with  $k$  projections for each point  $P_k$  at a time  $t_j$  (Fig. 1). Followed by an averaging over all  $k$  projections. Instead of simulating the intra-scan motion in the projection domain, we propose an alternative approach by convolving the reconstruction

with a respective motion kernel that depends on the systems exposure time. The projection  $p(s, \theta)$  for 2D parallel-beam can be described with

$$\rho(s, \theta) = \int_{-\infty}^{\infty} \int_{-\infty}^{\infty} f(x, y) \delta(x \cos \theta + y \sin \theta - s) dx dy \quad (1)$$

which is also called the Radon transform and is denoted by  $\mathbf{R}$  in the following [8]. The object density function  $f(x, y)$  can be reconstructed by a convolution with the filter kernel  $h(s)$  and a subsequent backprojection

$$f(x, y) = \int_0^{\pi} \int_{-\infty}^{\infty} p(s - t, \theta) h(t) dt d\theta \quad (2)$$

which is in the following denoted by  $\mathbf{R}^{-1}$  as the inverse Radon transform. As stated, the motion corrupted projection  $\hat{\rho}(s, \theta)$ , with the offsets  $s_{i,x}$  and  $s_{i,y}$  in  $x$  and  $y$ -direction, can be modeled as a weighted sum over  $l$  projections

$$\hat{\rho}(s, \theta) = \sum_{i=1}^l \omega_i \mathbf{R} \{ f(x - s_{i,x}, y - s_{i,y}) \} \quad (3)$$

Thus, the motion corrupted reconstruction  $\hat{f}(x, y)$  is

$$\hat{f}(x, y) = \mathbf{R}^{-1} \left\{ \sum_{i=1}^l \omega_i \mathbf{R} \{ f(x - s_{i,x}, y - s_{i,y}) \} \right\} \quad (4)$$

using the linearity of the inverse Radon transform, the weighted sum can be pulled out

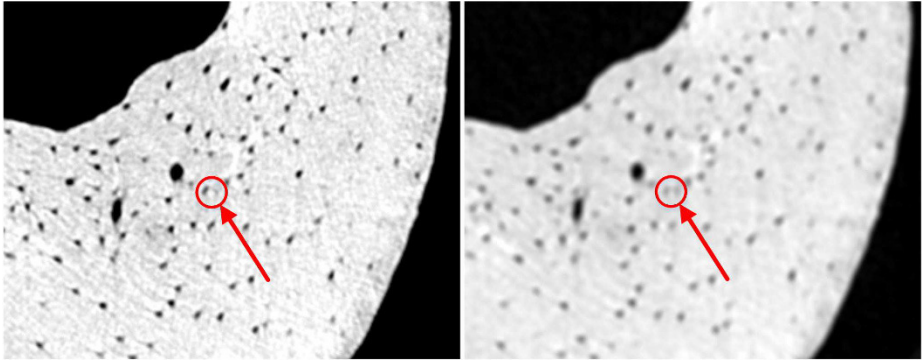
$$\hat{\rho}(s, \theta) = \sum_{i=1}^l \omega_i \mathbf{R}^{-1} \{ \mathbf{R} \{ f(x - s_{i,x}, y - s_{i,y}) \} \} \quad (5)$$

Using the property that Radon transform followed by its inverse cancel out, we obtain

$$\hat{\rho}(s, \theta) = \sum_{i=1}^l \omega_i f(x - s_{i,x}, y - s_{i,y}) \quad (6)$$

which is just the discrete formulation of a convolution of  $f(x, y)$  with some filter kernel  $\omega$ . Therefore by varying the number of projections  $l$ , we can simulate the strength of the motion during the acquisition of one projection. The filter kernels are created based on the concept shown in Fig. 1. For the currently used exposure time we consider all points, while for the higher frame rates we decrease the number of points.

**Fig. 2.** Reconstruction images of a mouse tibia. GT (left) and motion corrupted reconstruction due to respiration and muscle relaxation (right).



### 3 Results

Fig. 2 shows zoomed regions of the ground truth (GT) and the motion corrupted reconstruction, which includes breathing as well as motion due to the muscle relaxation. Motion blur is introduced in the motion corrupted image. Further, the shape and the position of the tiny bone structures changes, which is indicated with the arrow in both images. Additionally, ghost points appear in the marked area. Besides the qualitative evaluation, we obtain an SSIM of 0.732 for the motion corrupted image compared to the GT. The results of the exposure time variation experiment are shown in Fig. 3. All results are compared to the GT (a) using the SSIM. As can be seen, the SSIM values improve from 0.963 for a frame rate of 1 fps to an SSIM of 1.0 if frame rate of 32 fps is used.

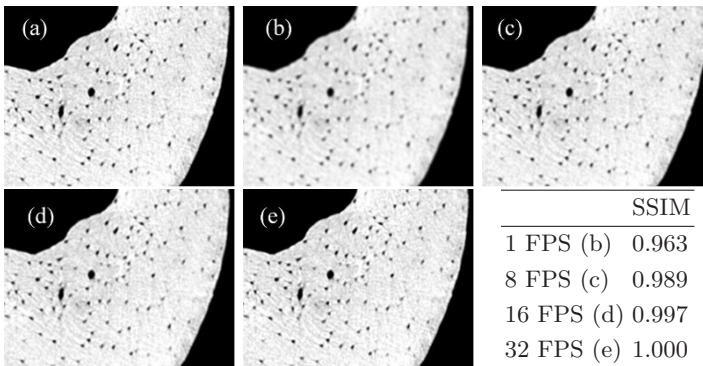


**Fig. 3.** The effect of respiration motion on reconstructed images simulated for different frame rates. Ground truth (a), 1 fps (b), 8 fps (c), 16 fps (d) and 32 fps (e) are compared in the table by means of the SSIM.

## 4 Discussion

In this work, we evaluate the impact of in-vivo mouse motion on the projection as well as the reconstructed image quality. We simulate motion and differentiate between inter- and intra-projection motion, which introduces blurring and motion artifacts in the reconstructions. These artifacts make diagnostics of the bony structure unfeasible. The result of the inter-scan muscle relaxation motion simulation shows the appearance of ghost points in the reconstruction images, which decreases the quality of the reconstructed bony structure. However, as muscle relaxation motion occurs as intra-projection movement, due to its slow velocity of  $10 \mu\text{m}$  per hour, this motion can be estimated and compensated by state-of-the-art motion correction methods. In contrast, the blurring effect of the breathing motion is a result of an average over multiple projections. This averaging is not invertible, thus we cannot compensate for the intra-scan motion. In the simulation evaluating the effect of the fps of the detector, we can observe that the reconstruction quality increases with the fps. This can be explained by looking at the strength of the breathing motion and the system setup. The assumed breathing motion with  $5 \mu\text{m}$  for a single breathing cycle and 4 cycles in a second lead to a movement of  $0.625 \mu\text{m}$  for a single projection using a detector with 32 fps. Since our detector has a spacing of  $1.34 \mu\text{m}$  the motion is not detectable in one projection. However, using a detector with 32 fps the breathing motion occurs between the acquisition and is therefore shifted towards an inter-scan motion, which is also compensatable with state-of-the-art motion correction methods. With the proposed simulation we have shown that in-vivo x-ray nanoscopy is feasible given that the frame rate of the detector is high enough such that all motion occurs as inter-scan motion and thus can be corrected. Motion correction itself is subject of our future work.

## References

1. Berger M, Xia Y, Aichinger W, et al. Motion compensation for cone-beam CT using fourier consistency conditions. *Phys Med Biol.* 2017;62(17):7181.
2. Bier B, Aichert A, Felsner L, et al.. Epipolar consistency conditions for motion correction in weight-bearing imaging. Springer; 2017.
3. Bier B, Unberath M, Geimer T, et al.; Springer. Motion compensation using range imaging in C-Arm cone-beam CT. *Proc MIUA.* 2017; p. 561–570.
4. Maier A, Hofmann HG, Berger M, et al. CONRAD: a software framework for cone-beam imaging in radiology. *Med Phys.* 2013;40(11):111914–1–8.
5. Kak AC, Slaney M. Principles of computerized tomographic imaging. Piscataway, NJ, United States: IEEE Service Center; 1988.
6. Parker DL. Optimal short scan convolution reconstruction for fanbeam CT. *Med Phys.* 1982;9(2):254–257.
7. Rohkohl C, Lauritsch G, Nöttling A, et al. C-Arm CT: Reconstruction of dynamic high contrast objects applied to the coronary sinus. *Proc IEEE NSS/MICR.* 2008; p. no pagination.
8. Zeng GL. Medical image reconstruction: a conceptual tutorial. Springer; 2010.